

**N89 - 15941**

**Optimal Post-Experiment Estimation  
of  
Poorly Modeled Dynamic Systems**

**D. Joseph Mook**

Department of Mechanical and Aerospace Engineering  
State University of New York at Buffalo  
Buffalo, New York 14260

**Abstract**

Recently, a novel strategy for post-experiment state estimation of discretely-measured dynamic systems has been developed. The method accounts for errors in the system dynamic model equations in a more general and rigorous manner than do filter-smoother algorithms. The dynamic model error terms do not require the usual process noise assumptions of zero-mean, symmetrically distributed random disturbances. Instead, the model error terms require no prior assumptions other than piecewise continuity. The resulting state estimates are more accurate than filters for applications in which the dynamic model error clearly violates the typical process noise assumptions, and the available measurements are sparse and/or noisy. Estimates of the dynamic model error, in addition to the states, are obtained as part of the solution of a two-point boundary value problem, and may be exploited for numerous reasons. In this paper, the basic technique is explained, and several example applications are given. Included among the examples are both state estimation and exploitation of the model error estimates.

PRECEDING PAGE BLANK NOT FILMED

## 1.0 Introduction

A large number of applications exist in the general area of "post-experiment" or "post-flight" estimation, wherein estimates of the state histories of a dynamic system are obtained using an assumed state dynamic model and sets of discrete measurements. In general, both the assumed model and the available measurements are imperfect. The motivation for applying an "optimal estimation" algorithm is to combine the model output with the available measurements in such a way as to obtain estimates of the state histories which are superior to both the model and the measurements, and, in addition, satisfy an optimality criterion. In this paper, a new estimation strategy is described which includes both a new optimality criterion and a new algorithm for obtaining estimates based on this condition.

The following generic problem statement for post-experiment estimation of a dynamic process is used to motivate the discussion. Given a system whose state vector dynamics is modeled by the (linear or nonlinear) system of equations,

$$\dot{\underline{x}} = \underline{f}[\underline{x}(t), \underline{u}(t), t] \quad (1)$$

where

$$\begin{aligned} \underline{x} &\equiv n \times 1 \text{ state vector} \\ \underline{f} &\equiv n \times 1 \text{ vector of model equations} \\ \underline{u} &\equiv p \times 1 \text{ vector of forcing terms,} \end{aligned}$$

and given a set of discrete measurements modeled by the (linear or nonlinear) system of equations,

$$\underline{\tilde{y}}(t_k) = \underline{g}_k[\underline{x}(t_k), t_k] + \underline{v}_k, \quad k = 1, \dots, m \quad (2)$$

where

$$\begin{aligned} \underline{\tilde{y}}(t_k) &\equiv r \times 1 \text{ measurement set at } t_k \\ \underline{g} &\equiv r \times 1 \text{ measurement model equations} \\ m &\equiv \text{total number of measurement sets} \\ \underline{v}_k &\equiv r \times 1 \text{ measurement error vector,} \end{aligned}$$

and  $\underline{v}_k$  is assumed to be a zero-mean, gaussian random sequence of known covariance  $R_k$ , determine the optimal estimate for  $\underline{x}(t)$  (denoted by  $\hat{\underline{x}}(t)$ ), during some specified time interval  $t_0 \leq t \leq t_f$ . Clearly, the definition of optimal is subjective, and we begin by discussing optimality criteria.

## 2.0 Optimality Criteria

The typical approach for obtaining an optimal estimate of the system state trajectories is the minimization of a function of the estimate error,

$$\epsilon_{\hat{\underline{x}}} \equiv E\{(\hat{\underline{x}} - \underline{x})\} \quad (3)$$

or its covariance,

$$P_{\hat{\underline{x}}\hat{\underline{x}}} \equiv E\{(\hat{\underline{x}} - \underline{x})(\hat{\underline{x}} - \underline{x})^T\} \quad (4)$$

Among these criteria are the well-known "maximum likelihood" and "minimum variance" strategies (e.g., Gelb<sup>1</sup>). For example, the minimum variance criterion requires the minimization of the trace of  $P_{\hat{\underline{x}}\hat{\underline{x}}}$ . Many other criteria which rely on estimating the estimate error statistics (Eqs. (3), (4)) have also been used as bases for estimation algorithms. A practical problem arises during actual

implementation of these methods. In order to determine the estimate error statistics, it is necessary to assume that any errors in the system model Eq. (1) are noise of known probability distribution. Most often, the probability distribution is assumed to be zero-mean gaussian, whose covariance is treated as a known quantity ("process noise"). The state estimation proceeds without any adjustment to the system model equations.

In general, it is difficult, if not impossible, to rigorously justify process noise assumptions for the model error. For real physical systems, error is likely to be due to modeling simplifications such as linearization, neglect of higher-order terms, etc., or, perhaps, just plain ignorance. Many of these likely sources are deterministic and non-zero mean. Consequently, the estimate error statistics in Eqs. (3) and (4) cannot be calculated rigorously. Estimates based on their optimization are sub-optimal, e.g., the minimum variance estimate is not truly minimum variance if the variance which is minimized is not the true variance.

These observations are well-known and are repeated here only to motivate the discussion. The optimal estimation strategies which require process noise assumptions work well in many applications, whether or not the model error assumption is justifiable, and filter algorithms are the most commonly used estimators in practice. The filters must generally be artistically "tuned", but this is often possible and sufficient for a reasonably accurate estimate.

However, filter accuracy may deteriorate substantially under a number of conditions. The filter algorithms rely on the integration of the original dynamic model Eq. (1) for the between-measurement estimate. If the model is poor and the measurements are sparse, the accumulated integration error between measurements may become very large. Even if the measurements are dense, if they are particularly noisy, and the model is poor, then the filter estimate may be of poor accuracy. Under certain conditions, the filter may become unstable. Divergence of filters when process noise assumptions are violated may be found in Fitzgerald<sup>2</sup>, Huber<sup>3</sup>, and Breza and Bryson<sup>4</sup>, among others.

With this motivation, Mook and Junkins<sup>5</sup> developed a new estimation strategy which eliminates any *a priori* assumptions about the model error except that it is continuous between the measurement times. The method, called Minimum Model Error (MME) estimation, is based on an optimality criterion which does not require estimation of the estimate error statistics, Eqs. (3)-(4). In the remainder of this paper, a summary of the method is given, followed by several application examples.

### 3.0 The Covariance Constraint Optimality Criterion

In the MME, a novel optimality criterion is used. The probability distribution of the state estimate error is not estimated. Instead, the optimal state trajectory estimate is determined on the basis of the assumption that the measurement-minus-estimate error covariance matrix must match the measurement-minus-truth error covariance matrix. This condition is referred to as the "covariance constraint". The covariance constraint is defined mathematically by requiring the following approximation to be satisfied:

$$\left\{ [\underline{\tilde{y}}(t_j) - \underline{g}(\underline{\hat{x}}(t_j), t_j)] [\underline{\tilde{y}}(t_j) - \underline{g}(\underline{\hat{x}}(t_j), t_j)]^T \right\} \approx R_j \quad (5)$$

Thus, the *estimated measurements*  $\underline{g}(\underline{\hat{x}}(t_j), t_j)$  are required to fit the *actual measurements*  $\underline{\tilde{y}}(t_j)$  with approximately the same error covariance as the actual measurements fit the truth. An algorithm for obtaining the estimates is described shortly.

The covariance constraint may be evaluated without knowledge of the estimate error statistics. Consequently, there is no need for process noise-like assumptions for the model error. In the next section, an algorithm which produces estimates which satisfy the covariance constraint is derived, treating model error as an unknown which is estimated along with the states.

The interpretation of the "approximately equal" sign in the covariance constraint may be adjusted according to the particular application. If the measurements are repeated samples of the same quantities, as is usual in a filtering problem, then a good approach is to calculate the covariance of the measurement-minus-estimate residuals using all of the measurements simultaneously. Thus, the covariance constraint is averaged over all of the measurements. In problems where several distinct sets of measurements are repeated, each set may be averaged separately. An example is spacecraft navigation, where the measurements may include sets of attitude measurements and sets of angular velocity measurements. These two sets are normally taken independently and contain different noise levels, so they should be averaged separately.

#### 4.0 MME Algorithm

If the dynamic model Eq. (1) contains significant error, then its output generally cannot predict the measurements with enough accuracy to satisfy the covariance constraint. The estimated measurement set at time  $t_k$  is based on the current state estimate,  $\hat{x}(t_k)$ , as shown in Eq. (2). The between-measurement state estimate is based on integration of the system dynamic model. Thus, if the system dynamic model contains errors, the integration does not yield the correct state estimate, and the residuals between the estimated and the actual measurements are too large. Consequently, the model error must be reduced in order to satisfy the covariance constraint. To accomplish this, a model correction term  $\underline{d}(t)$  is added to the original dynamic model as

$$\dot{\underline{x}} = \underline{f}[\underline{x}(t), \underline{u}(t), t] + \underline{d}(t) \quad (6)$$

In general, an infinite number of  $\underline{d}(t)$ 's exist which are capable of correcting the model to satisfy the covariance constraint. The minimum correction is sought, thereby providing the least adjustment to the original model. Accordingly, the following cost functional is minimized with respect to  $\underline{d}(t)$ :

$$J = \sum_{j=1}^m \left\{ [\underline{y}(t_j) - \underline{g}(\hat{\underline{x}}(t_j), t_j)]^T R_j^{-1} [\underline{y}(t_j) - \underline{g}(\hat{\underline{x}}(t_j), t_j)] \right\} + \int_{t_0}^{t_f} \underline{d}^T(\tau) W \underline{d}(\tau) d\tau \quad (7)$$

where  $W$  is a  $k \times k$  weight matrix chosen to satisfy the covariance constraint as described shortly. The functional  $J$  in Eq. (7) is the sum of two penalty terms, whose relative weighting is controlled by  $W$ . If  $W$  is near zero, then the integral term is nearly zero. Consequently, the allowable  $\underline{d}(t)$  is virtually unlimited and thus the model is corrected until the measurements are predicted almost exactly (i.e., the summation term goes to zero). However, this is only appropriate when the measurements are perfect. If the measurements are noisy, then the covariance constraint implies that the summation term should not be zero. The weight matrix,  $W$ , is chosen such that the covariance constraint is satisfied, allowing just enough correction  $\underline{d}(t)$ . Generally, determination of  $W$  requires a search procedure. However, unlike the tuning of a filter, which is essentially artistic,  $W$  is specified by satisfaction of the covariance constraint.

In Figure (1), the concept of the covariance constraint is demonstrated for a one-dimensional ( $n=1$ ) system. Figure (1a) shows the ratio of the left-hand side of Eq. (5) to the right-hand

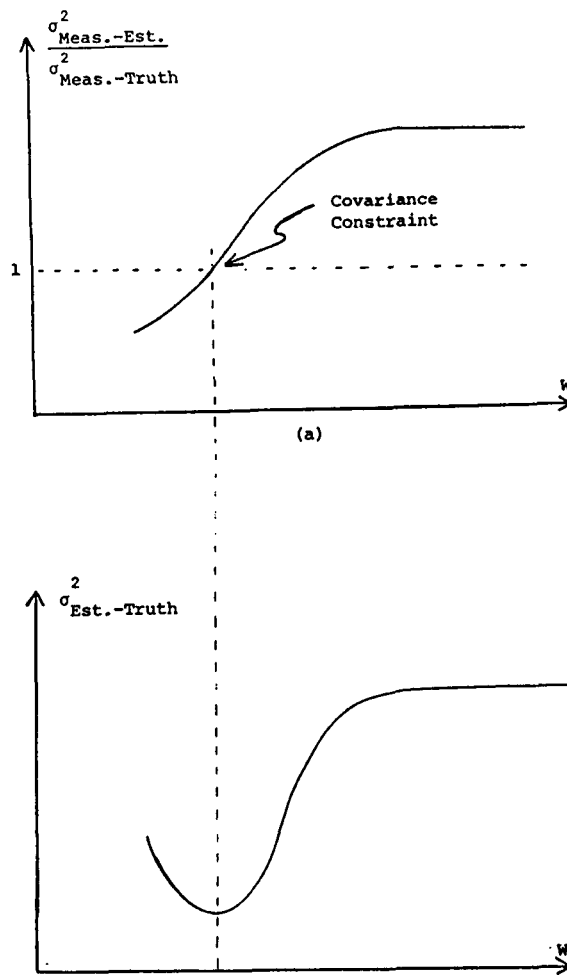


Figure 1. Choosing  $W$  to satisfy the covariance constraint leads to the optimal state estimate.

side, plotted versus  $W$ . As the weight is decreased, the corrected model predicts the actual measurements more closely as shown in the figure. In Figure (1b), the estimate variance is plotted versus  $W$ . The covariance constraint implies that the optimal estimate occurs when the covariance constraint is satisfied.

An algorithm for the minimization of  $J$  in Eq. (7) follows directly from a modification (e.g., Geering<sup>6</sup>) of the so-called Pontryagin's necessary conditions (e.g., Rozonoer<sup>7</sup>). For a given  $W$ , the minimization of  $J$  in Eq. (7) with respect to  $\underline{d}(t)$  leads to the two-point boundary value problem (TPBVP) summarized as:

$$\dot{\underline{x}} = \underline{f}[\underline{x}(t), \underline{u}(t), t] + \underline{d}(t) \quad (6)$$

$$\dot{\underline{\lambda}} = - \left( \frac{\partial \underline{f}}{\partial \underline{x}} \right)^T \underline{\lambda} \quad (8)$$

$$\underline{d} = - \frac{1}{2} W^{-1} \left[ \frac{\partial \underline{f}}{\partial \underline{u}} \right]^T \underline{\lambda} \quad (9)$$

$$\underline{x}(t_0) = \text{specified, or } \underline{\lambda}(t_0^-) = \underline{0} \quad (10)$$

$$\underline{\lambda}(t_j^+) = \underline{\lambda}(t_j^-) + 2H_j^T R_j^{-1} [\underline{y}(t_j) - \underline{g}(\underline{\hat{x}}(t_j), t_j)] \quad (11)$$

$$\underline{x}(t_f) = \text{specified, or } \underline{\lambda}(t_f^+) = \underline{0} \quad (12)$$

where

$$H \equiv \left. \frac{\partial \underline{g}}{\partial \underline{x}} \right|_{\underline{\hat{x}}(t_j), t_j}$$

This TPBVP contains jump discontinuities in the costates at each measurement time where the predicted measurement does not exactly match the actual measurement. The size of the jump is proportional to the measurement residual  $[\underline{y}(t_j) - \underline{g}(\underline{\hat{x}}(t_j), t_j)]$ , which, via the covariance constraint, is proportional to the measurement noise. From Eq. (9), these costate jumps lead to jumps in the estimated model error. Thus, for noisy measurements, the model error estimates are jump discontinuous proportional to the measurement residuals. Note that this is identical to a filter except that in a filter, the jumps are in the state estimates. The MME state estimates are continuous.

The algorithm Eqs. (6)-(12) exhibits several desirable features of both batch and sequential estimation techniques. The state estimate is obtained by processing all of the available measurements, much like a batch estimator such as least squares. Thus, the estimate is optimized in a *global* sense. In addition, the state estimate is continuous, eliminating the jump discontinuities present in filter estimates. For many physical systems, jump discontinuities in the states are not possible; thus, jump discontinuities in the filter state estimates must be reconciled in an artful manner. In addition to the batch algorithm-like advantages, the minimum model error algorithm calculations are based upon sequential processing of the measurements, which, like the filter algorithms, greatly reduces the memory requirements and eliminates the need for large matrix manipulations. From the standpoint of algorithmic calculations, the minimum model error technique shares advantages of both batch and sequential estimation techniques.

If the assumed model in the MME algorithm is linear, then a multiple shooting technique may be used to solve the TPBVP described by Eqs. (6)-(12) (Lew and Mook<sup>8</sup>). This technique converts the TPBVP into a set of linear algebraic equations which may be solved using any linear equation solver.

When the covariance constraint has been satisfied, the estimate is considered to have been optimized. As a byproduct of the solution, the estimates  $\underline{d}(t)$  of the model error required to satisfy the optimality criterion are available. The results of the examples clearly indicate that these terms may provide highly accurate estimates of the actual model errors, leading to potential improvements in the model.

## 5.0 Examples

In this section, several example applications are summarized which demonstrate the present method and explore the accuracy of both the state estimates and the model error estimates obtained using it. The examples include both linear and nonlinear systems, varying degrees of model error, varying levels of measurement noise, measurement frequency, and total number of measurements. Exploitation of the model error estimates is also demonstrated.

## 5.1 Simple Example of Minimum Model Error Estimation

To illustrate the application of the minimum model error approach, consider estimation of a scalar function of time for which noisy measurements are the only information available. No prior knowledge of the underlying dynamics is assumed. Thus, the system dynamic model equation is

$$\dot{x} = 0 \quad (13)$$

Using the minimum model error approach, the system model is modified by the addition of a to-be-determined unmodeled effect as

$$\dot{x} = 0 + d(t) \quad (14)$$

where  $d(t)$  represents the dynamic model error. For simplicity, the measurements are direct measurements of the state itself, and the measurement noise is a zero mean gaussian process with a variance of  $\sigma^2$ , given as

$$\tilde{x}(t_k) = x(t_k) + v_k, \quad k = 0, \dots, m \quad (15)$$

where  $\tilde{x}_k$  is the measurement at time  $t_k$ ,  $x_k$  is the true state at time  $t_k$ , and  $v_k$  is a zero-mean gaussian sequence of variance  $\sigma^2$ . The cost functional to be minimized (see Eq. (7)) is

$$J = \frac{1}{\sigma^2} \sum_{k=0}^m [\tilde{x}(t_k) - \hat{x}(t_k)]^2 + \int_{t_0}^{t_m} d^2(\tau) W d\tau \quad (16)$$

where  $W$  is the to-be-determined weight on the integral sum-square model error term. The TPBVP which results from the minimization of  $J$  with respect to  $d(t)$  may be summarized as (see Eqs. (6)-(12))

$$\begin{aligned} d &= -\frac{\lambda}{2W} \\ \dot{x} &= d = -\frac{\lambda}{2W} \\ \dot{\lambda} &= -\frac{\partial f}{\partial x} \lambda = 0 \\ \lambda(t_0^-) &= \lambda(t_f^+) = 0 \\ \lambda(t_k^+) &= \lambda(t_k^-) + \frac{2}{\sigma^2} (\tilde{x}_k - \hat{x}_k) \end{aligned}$$

where  $\underline{\lambda}$  is the vector of costates. The boundary conditions indicate that the state is unknown at  $t_0$  or  $t_f$ . The algorithm proceeds according to the following steps:

- 1) Choose  $W$
- 2) Solve the TPBVP
- 3) Check the covariance constraint
- 4) If the covariance constraint is not satisfied, go to step 1

The true state history for this example is taken as  $x(t) = \cos(t)$ . In Fig. 2, a set of 101 simulated measurements spanning the time interval  $t_0 = 0$  to  $t_f = 10$  is shown. The measurements were simulated by adding a computer-generated gaussian random sequence to the true state as

$$\tilde{x}_k = \cos(t_k) + v_k \quad (17)$$

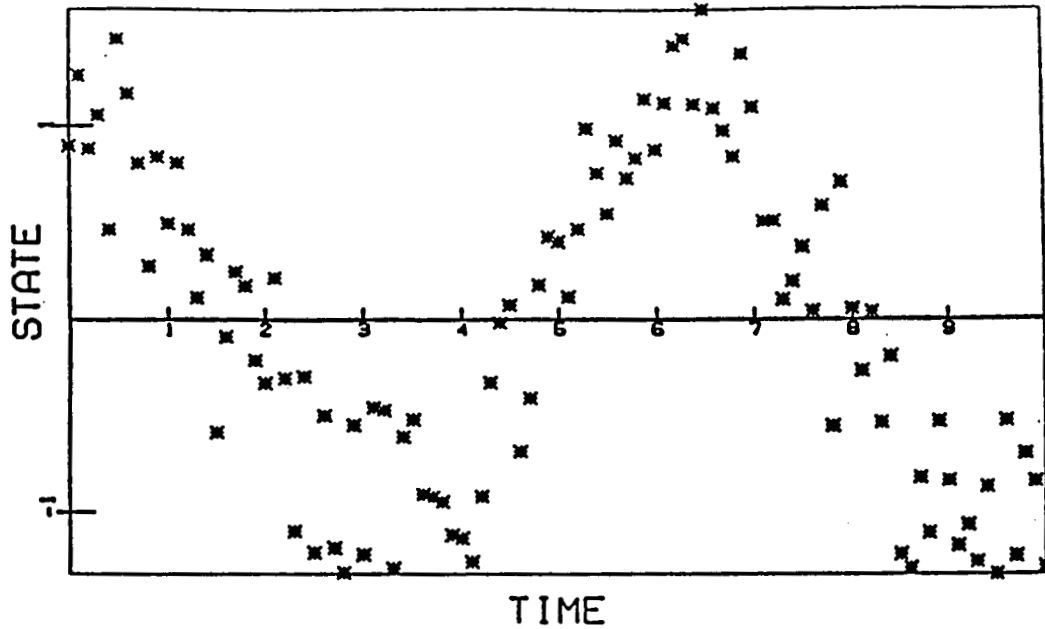


Figure 2. Simulated measurements of  $\cos(t)$  with  $\sigma^2 = 0.114$ .

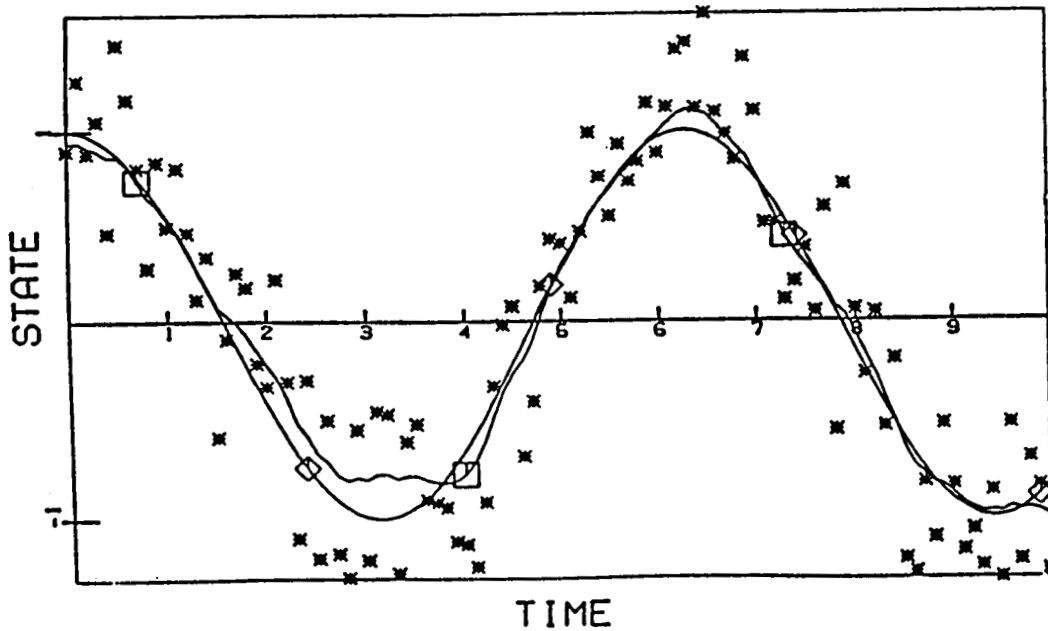


Figure 3. MME estimates using the Figure (2) measurements with no model. \* denotes measurement,  $\diamond$  denotes truth ( $\cos(t)$ ),  $\square$  denotes MME estimate.

The nominal variance of  $v_k$  in Fig. 2 is 0.1, although the actual variance depends on the seed supplied to the random number generator. This variance is 10% of the peak amplitude. Thus, the average measurement error is approximately 50% of the average amplitude.

In Fig. 3, the minimum model error state estimate is shown along with the measurements



and the true state history. Note that the state has been reconstructed to an error variance of .0085, considerably better than the measurement variance even in the total absence of a model. Note also that the model prediction variance (i.e., constant  $x = 0$ ) is 0.717.

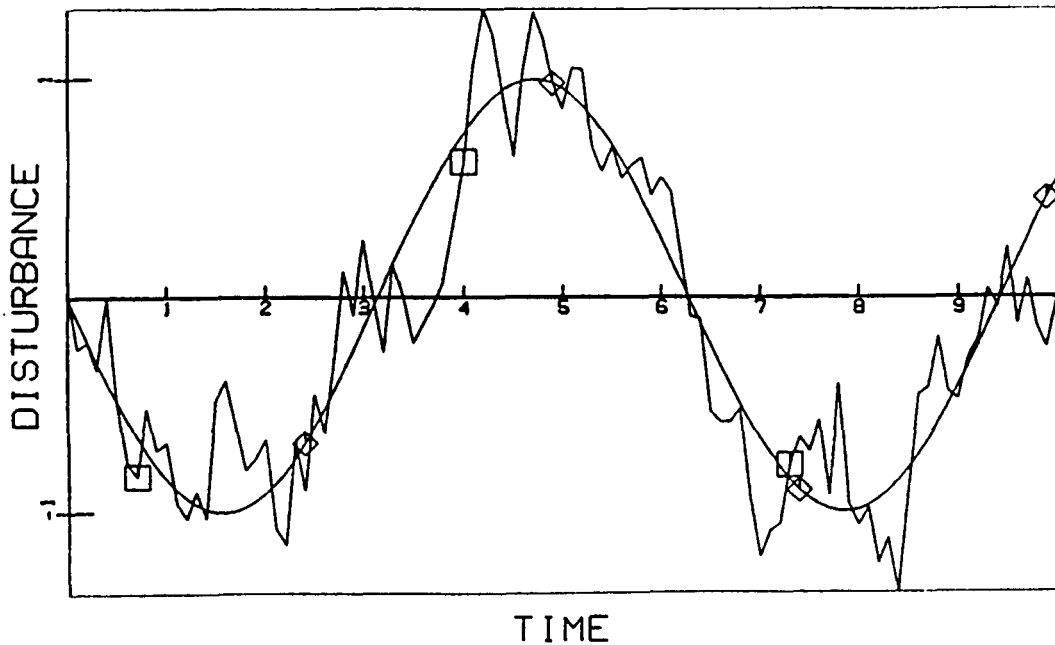


Figure 4. MME model error estimates using the Figure (2) measurements with no model.  $\diamond$  denotes true model error ( $-\sin(t)$ ),  $\square$  denotes MME estimate.

In Fig. 4, the model error term is plotted along with the true model error,  $-\sin(t)$ . Although the model error estimate contains considerable noise, due to the noisy measurements, it is an accurate representation of the actual model error. Based on an examination of Fig. 4, a user might easily conclude that the dynamic model error is indeed  $-\sin(t)$ . If the dynamic model is amended from  $\dot{x} = 0$  to  $\dot{x} = -\sin(t)$ , and the estimation process repeated, the state estimate is virtually exact and the model error estimate is virtually zero.

## 5.2 System State Estimation from MME

Several applications examples are now presented for system state estimation using the MME method. Other examples have also been investigated but are omitted here due to space limitations.

### 5.2.1 Modal Space State Estimation

In these examples, taken from Mook and Lin<sup>9</sup> and Lin<sup>10</sup>, the state histories of the output measurements of a system described by a linear sum of system modes are obtained using the MME. The simulated measurements are created by assuming a truth as a sum of several modes, and then adding gaussian noise to the truth. The assumed model for the MME estimation is taken as the first mode in the sum. All of the other modes are ignored in the assumed model. Figures (5) shows the results from a case with a five mode truth. The one-mode model is plotted along with the MME estimate and the truth. The model is seen to be very poor, but the estimate is essentially perfect. The measurement noise is gaussian with  $\sigma^2 = 0.04$ , and the measurement interval is 0.1

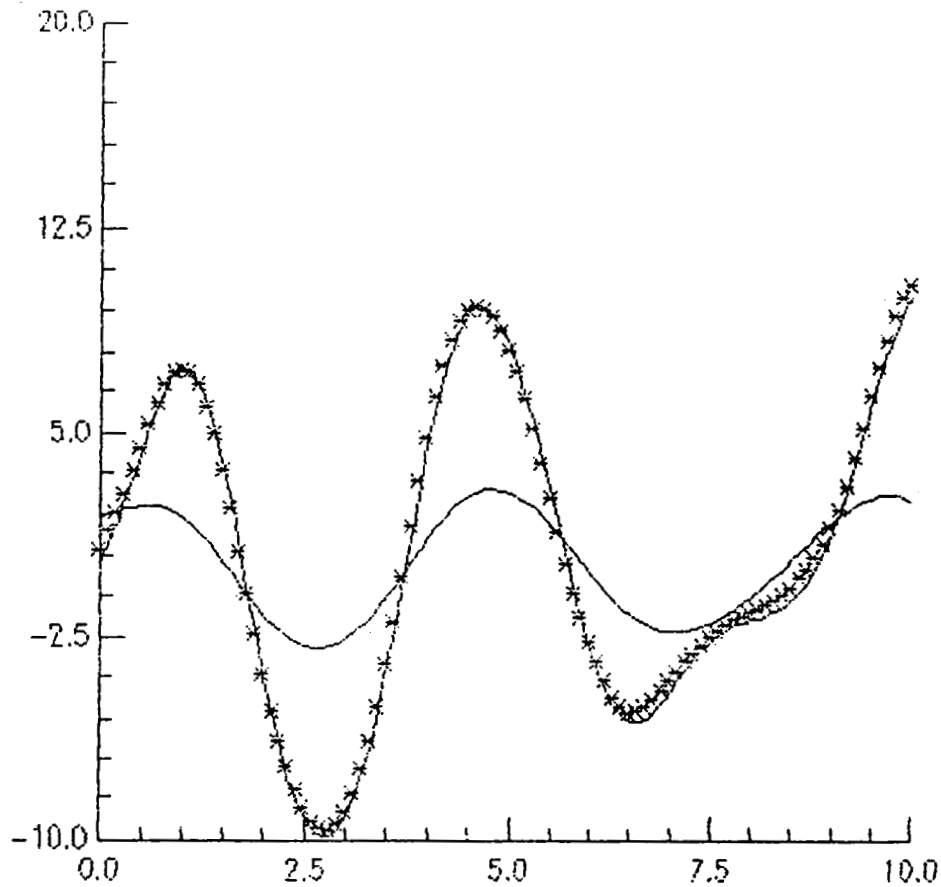


Figure 5. One-mode assumed model, five-mode truth, and MME estimate (\*).

seconds.

Clearly, the MME is able to recover from a very poor model to produce accurate state estimates. This result can be very helpful for structural modelers who are uncertain about whether or not a modal model has been truncated with the correct number of retained modes.

### 5.2.2 Nonlinear State Estimation

The following example is taken from Mook<sup>11</sup>. Consider the single-degree-of-freedom system modeled by

$$\ddot{x} + \omega_0^2 x = f(x(t), \dot{x}(t)) + F(t) \quad (18)$$

where  $x$  and  $\dot{x}$  are the system states,  $F(t)$  is a known external excitation, and  $f(x(t), \dot{x}(t))$  contains terms which may be nonlinear in the states. The external excitation is assumed to be independent of the states. Eq. (18) may be converted to state-space form as

$$\dot{z} = \begin{pmatrix} 0 & 1 \\ -\omega_0^2 & 0 \end{pmatrix} z(t) + \begin{pmatrix} 0 \\ F(t) \end{pmatrix} + \begin{pmatrix} 0 \\ f(x(t), \dot{x}(t)) \end{pmatrix} \quad (19)$$

where  $z \equiv \{x(t) \ \dot{x}(t)\}^T$ . A specific example, after Thompson and Stewart<sup>12</sup>, is given by

$$2.56\ddot{x} + 0.32\dot{x} + x + 0.05x^3 = 2.5\cos(t) \quad (20)$$

This example exhibits two distinct possible steady-state solutions, depending on the initial conditions. The assumed model for the MME algorithm is used in two different forms. First, the

nonlinear system is modeled for the MME as a linear oscillator. Measurements are simulated with a variety of different noise levels and frequencies. In each case, the MME is able to obtain accurate state estimates. Results are shown in Figures (6) through (8). In part (a) of each figure, the measurements are plotted along with the linear model output, thus showing the information given to the MME method. In part (b) of each figure, the truth, measurements, and MME estimate are shown. The accuracy of the state estimate is apparent from the figures, even for measurement frequency less than 4/cycle and total measurements as low as 15 (Figure (7)), and for noise levels with  $\sigma$  equal to 30% of the peak amplitude (Figure (8)).

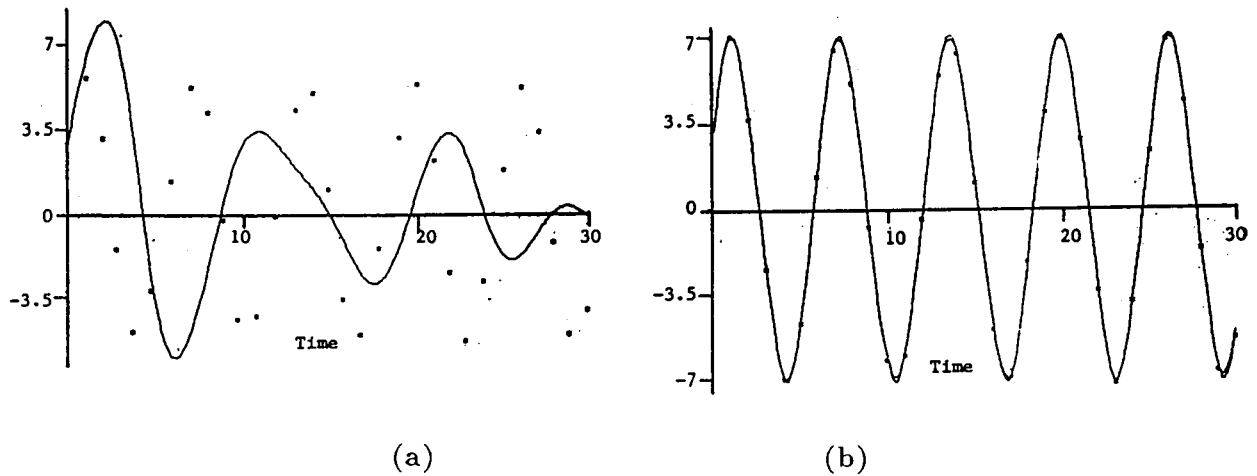


Figure 6. (a) Nonlinear estimation with 30 noiseless measurements, using assumed linear oscillator model. (b) Truth, measurements, and MME estimates.

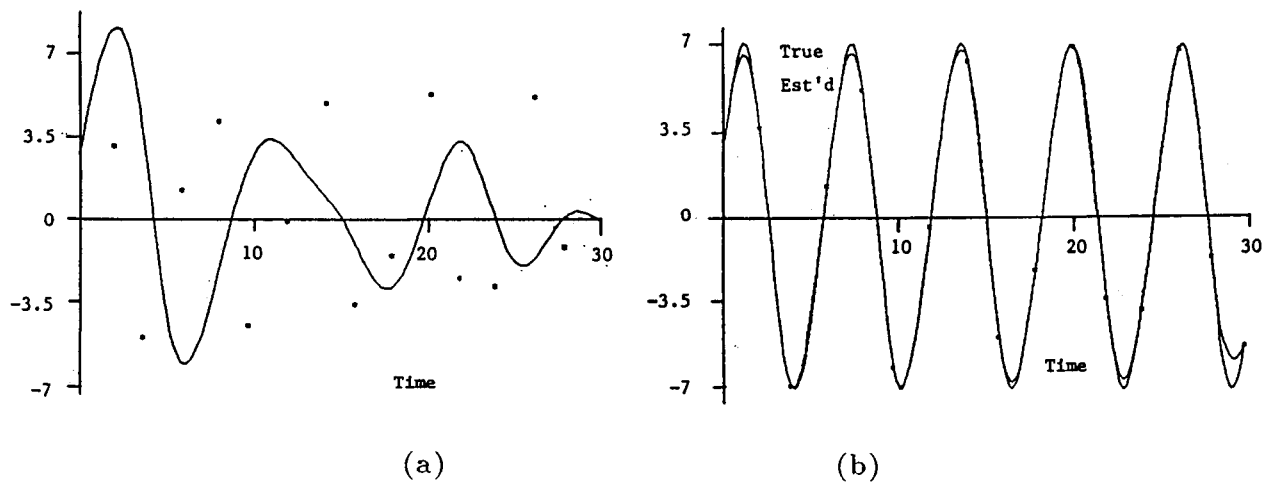


Figure 7. (a) Nonlinear estimation with 15 noiseless measurements, using assumed linear oscillator model. (b) Truth, measurements, and MME estimates.

Second, the assumed model for the MME consisted only of the external forcing, so that no knowledge of the system is assumed. Results are shown in Figure (9), where the MME estimate pictured in part (b) is seen to be very accurate despite the very poor model pictured in part (a).

ORIGINAL PAGE IS  
OF POOR QUALITY

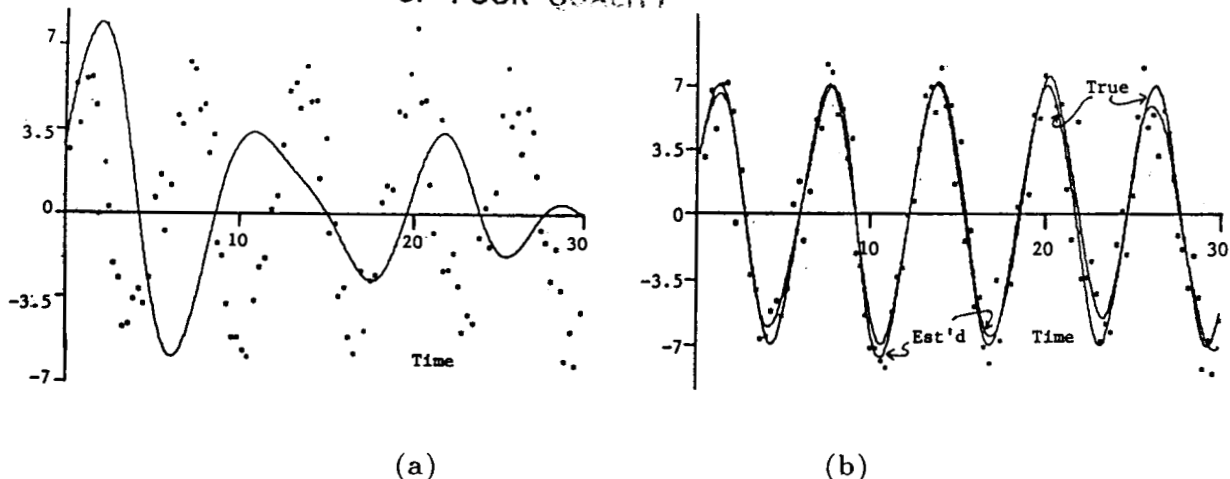


Figure 8. (a) Nonlinear estimation with 100 noisy measurements, with noise level approximately 30%. (b) Truth, measurements, and MME estimates.

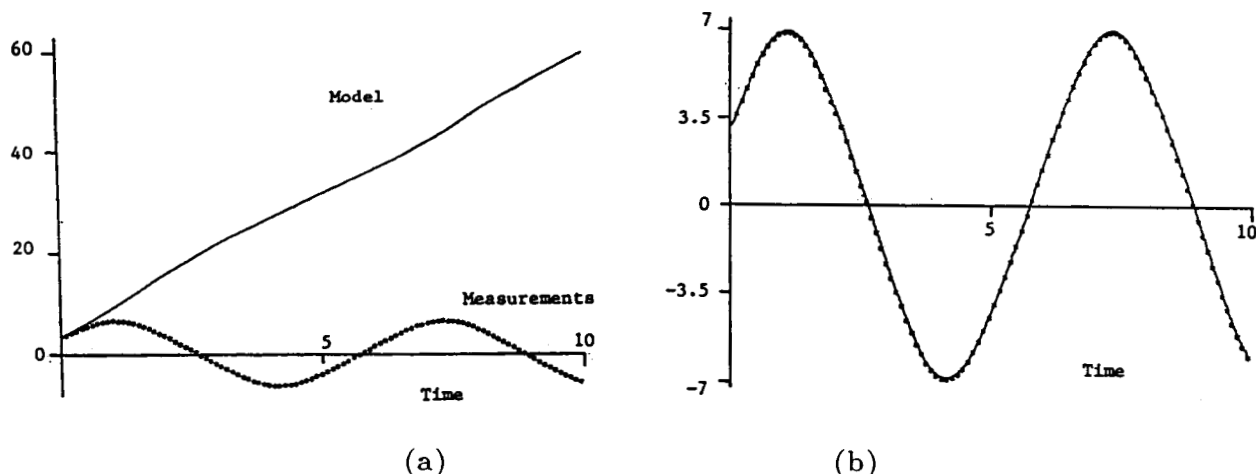
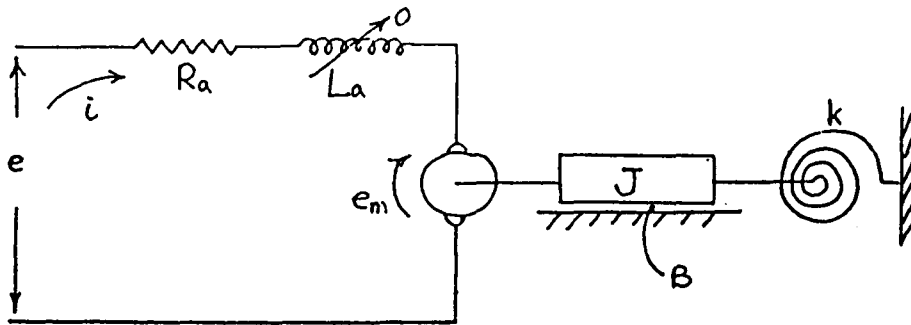


Figure 9. (a) Nonlinear estimation with 100 noiseless measurements, using no assumed model. (b) Truth, measurements, and MME estimates.

### 5.3 System Identification From Model Error Estimates

An area of considerable interest in many engineering disciplines is identification, the process of obtaining an accurate model of a dynamic process using measured data. State estimation and identification are most often two separate processes. Some versions of Kalman filters have been implemented which treat unknown constant processes in a model as states, so that they are estimated as part of the state vector. This approach, like most other identification techniques, requires the user to construct a model of appropriate form and order *a priori*. The filter then estimates the constant parameters in the model. However, the filters still assume that any model error is a gaussian white noise, so this approach usually works well only if the model order and form are correctly chosen by the user. The MME, by estimating the model error, may be used to determine the form of the model error before attempting to estimate the parameters.

Several studies have been conducted to investigate the use of the MME as an aid to system



$$\dot{z} = \begin{pmatrix} 0 & 1 \\ -\frac{K}{J} & -\frac{BR_a + K_T K_b}{JR_a} \end{pmatrix} z + \begin{pmatrix} 0 \\ \frac{K_T}{JR_a} \end{pmatrix} e$$

Figure 10. Armature-controlled motor drives a rotating shaft assembly with inertia  $J$ , damping  $B$ , and stiffness  $k$ . The motor constants are  $K_T$  and  $K_b$ , and  $z = \{\theta \dot{\theta}\}^T$ .

identification. These results are presented next.

### 5.3.1 Linear State Space Parameter Identification

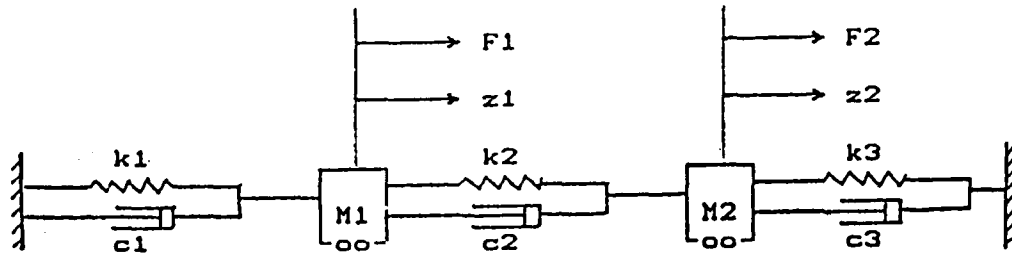
The simplest form of model to identify is the linear, time-invariant state-space model. This is also the most commonly used model form in practice. Some examples of linear system identification are given in Mook, Liu, and Ho<sup>13</sup>, and some results of that study are repeated here. Two assumed true systems are studied; an armature-controlled motor system driving a rotating shaft assembly, shown in Figure (10), and a linear, two-degree-of-freedom model nominally represented by two masses, springs, and dampers, as shown in Figure (11). In Figure (10), the term  $A_{22} = -\frac{BR_a + K_T K_b}{JR_a}$ , which represents damping, is assumed to be unknown and is to be estimated. In Figure (11), the three damper constants are to be estimated from the free response. Simulated measurements are created for both cases by adding gaussian white noise to the truth, and several cases are presented for varying noise, measurement frequency, and record length. In addition, the assumed model used for the MME is varied from case to case by altering the assumed values for the unknown constants.

The parameter estimation is carried out by a least-squares fit of the estimated model error. Since the model error estimate is continuous except at the measurement times, it may be sampled at an arbitrary number of points away from the measurements to create an overdetermined system of algebraic equations in the unknown parameters. Then, a least-squares algorithm is used to produce the parameter estimates. Results for the system in Figure (10) are shown in Table (1), and for the system in Figure (11), in Table (2).

### 5.3.2 Nonlinear System Identification

In section 5.2.2, results are given which demonstrate very accurate state estimation of a nonlinear system, given poor dynamic models and noisy, sparse data. In this section, identification results are given for those same examples. More detail is available in Mook<sup>11</sup>.

The model error estimates corresponding to Figures (6)-(9) are shown in Figures (12)-



$$\dot{z} = \begin{pmatrix} 0 & 1 & 0 & 0 \\ -(k_1 + k_2) & -(c_1 + c_2) & -k_2 & -c_2 \\ 0 & 0 & 0 & 1 \\ -k_2 & -c_2 & -(k_2 + k_3) & -(c_2 + c_3) \end{pmatrix} z + \begin{pmatrix} 0 \\ F_1 \\ 0 \\ F_2 \end{pmatrix}$$

Figure 11. Mass-spring-damper system, where  $F$  is applied force.

Table 1. Parameter estimates for the system in Figure (10).

Measurement Frequency (meas/10 sec)	Measurement Variance	True $A_{22}$	Estimated $A_{22}$	Error %
41	0.	-0.4	-0.4000	0.00
41	0.00018	-0.4	-0.394691	1.33
21	0.00014	-0.4	-0.395293	1.18
11	0.00015	-0.4	-0.415468	3.87
41	0.0045	-0.4	-0.361596	9.60

(15). Clearly, the model error estimates are dependent on the accuracy and frequency of the measurements. For more accurate and more frequent measurements, the model error estimates are smoother and more accurate. However, the accuracy of the model error is not dependent on the accuracy of the assumed model. This is a very significant result for identification.

In order to identify the nonlinear model from the model error estimates, a parameterized model of the model error is constructed and then the parameters are estimated using a least-squares algorithm. For demonstration purposes, the assumed model for identification contained more terms than the actual model error, including the case when no prior model is assumed for the MME (Figures (9) and (15)). The least squares fit produced near-zero parameter estimates for the assumed model error terms which are not in the model, and near-perfect parameter estimates for the assumed terms which are in the model.

Table 2. Parameter estimates for the system in Figure (11).

values of c's measurements	true	guess	estimate	error (%)
perfect	.2, .1, .3	0., 0., 0.	0.207	3.5
noisy			0.092	8.0
		0.291	3.0	
perfect		.4, .2, .6	0., 0., 0.	0.210
noisy	0.108			8.0
	0.278		8.0	
perfect	.4, .2, .6		0., 0., 0.	0.205
noisy		0.097		3.0
		0.286	4.6	
perfect		.4, .2, .6	0., 0., 0.	0.208
noisy	0.095			5.0
	0.277		7.7	

(values are in the order of c1, c2, c3)

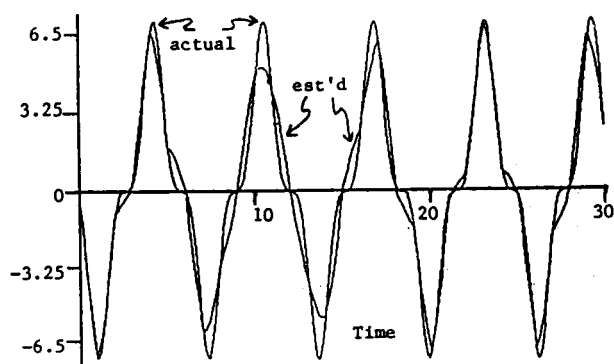


Figure 12. Model error estimation with 30 noiseless measurements, using assumed linear model.

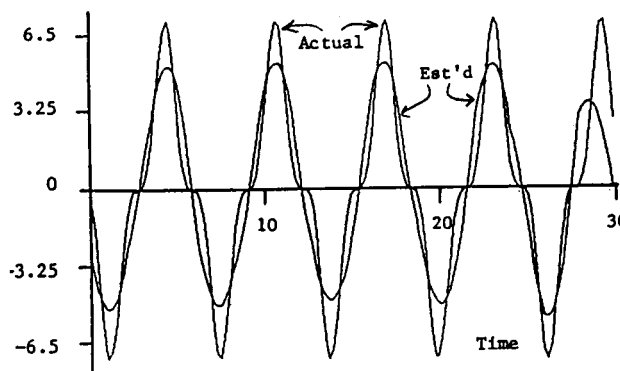


Figure 13. Model error estimation with 15 noiseless measurements, using assumed linear model.

### 5.2.3 Modal Space Realization/Identification

Recently, considerable interest in the identification of modal space models for large flexible systems has arisen in conjunction with such proposed projects as the space station. Several methods which produce accurate modal models from time-domain data have been developed (e.g., Ibrahim and Mikulcik<sup>14</sup>; Rajaram and Junkins<sup>15</sup>; Hendricks *et al*<sup>16</sup>; Chen *et al*<sup>17</sup>). The recently developed Eigensystem Realization Algorithm (Juang and Pappa<sup>18</sup>) is particularly attractive because it first determines the model order and then estimates the model parameters. This alleviates a very serious drawback of most methods, which require that the model order be known *a priori*. However, Juang and Pappa<sup>19</sup> found that for high noise levels in the measurements, the ERA could not determine the correct number of modes in the model, and the parameter estimates for the model were of low

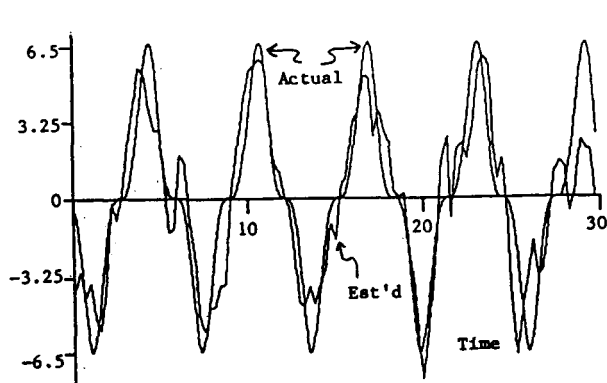


Figure 14. Model error estimation with 100 noisy measurements, using assumed linear model.

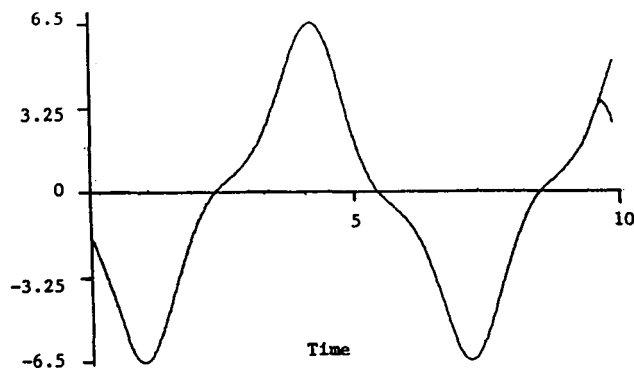


Figure 15. Model error estimation with 100 noiseless measurements, using no assumed model.

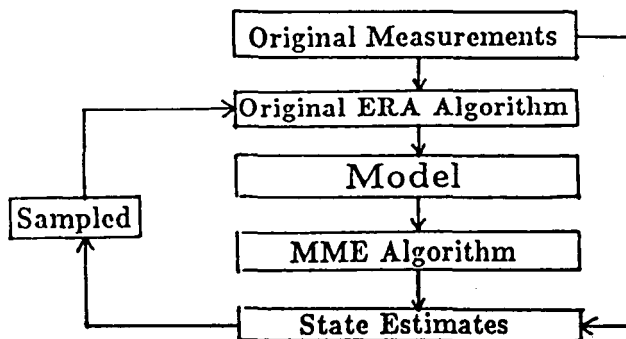


Figure 16. Algorithm flowchart for modal identification.

accuracy.

In Mook and Lew<sup>20</sup>, the MME method is used in conjunction with the ERA to produce an algorithm which is significantly less sensitive to noise. The algorithm may be summarized as (i) apply ERA to the original measurements, (ii) use the ERA-produced model and the original measurements in the MME to produce state estimates of the measurements, (iii) sample the MME-produced state estimates to create simulated measurements of higher accuracy than the original measurements, and (iv) apply ERA to the simulated measurements in order to realize/identify the correct model. The steps (ii)-(iv) may be repeated, since the MME will produce more accurate state estimates if a more accurate model is used. Consequently, if the first pass through steps (ii)-(iv) produces more modes than step (i), a second pass through steps (ii)-(iv) may further improve the accuracy of the realization/identification. The entire procedure is represented by the flowchart in Figure (16).

The combined algorithm has been investigated for identification of the modes of a clamped-clamped beam. The true model is given by

$$y(t) = 1.0\sin(t) + 0.05\sin(2.76t) + 0.001\sin(5.4t) \quad (21)$$

Measurement data was created with several noise levels, including  $\sigma = 0.001$ ,  $\sigma = 0.003$ ,  $\sigma = 0.01$ ,



$\sigma = 0.05$ , and  $\sigma = 0.1$ . Note that the highest noise level corresponds to approximately 10% of the measurement amplitude, while the lowest noise level is approximately 0.1% of the amplitude. Moreover, the highest noise level is twice as high as the second, and 100 times as high as the third, modal amplitudes, while the lowest noise level is equal to the smallest modal amplitude.

Table 3. Singular values from the ERA algorithm.

$\sigma = 0.1$	$\sigma = 0.05$	$\sigma = 0.01$	$\sigma = 0.003$	$\sigma = 0.001$	$\sigma = 0.0$
29.484	29.468	29.458	29.457	29.457	29.456
20.038	20.030	20.028	20.028	20.028	20.028
2.166	1.675	1.331	1.279	1.264	1.257
1.638	1.199	0.904	0.862	0.851	0.845
1.196	0.593	0.118	0.035	0.023	0.026
1.181	0.590	0.113	0.034	0.019	0.022
1.134	0.566	0.110	0.033	0.012	$10^{-12}$
1.124	0.561	0.108	0.031	0.011	$10^{-12}$
1.083	0.541	0.106	0.030	0.011	$10^{-13}$
1.031	0.516	0.102	0.029	0.010	$10^{-13}$
0.965	0.483	0.097	0.029	0.010	$10^{-13}$
0.942	0.471	0.094	0.028	0.009	$10^{-13}$

The model order is determined from the singular values of the singular value decomposition of  $H(0)$ , where  $H$  is the so-called "Hankel matrix". The model order is determined by the number of pairs of singular values between which there is a significant drop in magnitude. Table (3) gives the singular values in order from largest to smallest for each of the five noise levels. It appears that the model order is one, perhaps two, for  $\sigma = 0.1$ , since the singular value pairs beginning with the second pair are approximately the same magnitude. Consequently, for noise levels of  $\sigma = 0.1$ , the ERA method indicates one mode from the measurements. This seems intuitively reasonable since the level of noise exceeds the amplitude of modes 2 and 3.

Table 4. Parameter identification from the ERA algorithm.

Noise	Mode 1		Mode 2		Mode 3	
	Frequency	Damping	Frequency	Damping	Frequency	Damping
$\sigma = 0.1$	1.007	$-2.25 \times 10^{-2}$	2.473	-2.410	11.48	-31.44
$\sigma = 0.05$	1.013	$-1.37 \times 10^{-2}$	2.660	-0.967	12.87	-31.36
$\sigma = 0.01$	1.003	$-3.23 \times 10^{-3}$	2.739	-0.048	26.26	-10.54
$\sigma = 0.003$	1.001	$-8.37 \times 10^{-4}$	2.753	$2.11 \times 10^{-3}$	26.22	-10.45
$\sigma = 0.001$	1.000	$-3.14 \times 10^{-4}$	2.756	$3.18 \times 10^{-3}$	5.487	-4.27
True	1.000	0	2.760	0	5.400	0

After the model order is determined, the ERA algorithm estimates the modal frequencies and damping factors. Note that the true frequencies for this example are given in Eq. (21), and the

true damping factors are 0. The frequencies and damping factors estimated by the ERA method are given in Table (4), along with the true values. In constructing Table (4), we have chosen the number of modes as three in all cases, even though this is not clear from the singular values. The damping and frequency parameters in Table (4) clearly indicate that modes 2 and 3 have not been discerned from the noisier measurements.

We now proceed to apply the combined ERA/MME algorithm to the same five sets of measurements used in the ERA algorithm. The assumed dynamic model varies from case to case. The results from Tables (3) and (4) were used to construct the models which were assumed for the MME algorithm. Thus, for the three highest noise levels, the MME used only the first mode identified by the ERA, and for the lower two noise levels, used the first two modes identified by the ERA. The MME algorithm produced state estimates for the measurement position. These estimates were then sampled at the original measurement times to produce "simulated" measurements which contain significantly less noise than the original measurements. Finally, the ERA algorithm is again applied, this time to the simulated measurements. Although a second application of this procedure may improve the realization/identification, as illustrated in Figure (1), we present results for a single pass only. The singular values obtained by ERA processing of the sampled MME estimates are given in Table (5). These singular values indicate three modes for every noise level. The parameter identification results are given in Table (6). All three frequencies are identified at all noise levels. The damping identification for the first two modes is also very good at all noise levels.

Table 5. Singular values from the ERA/MME algorithm.

$\sigma = 0.1$	$\sigma = 0.05$	$\sigma = 0.01$	$\sigma = 0.003$	$\sigma = 0.001$	$\sigma = 0.0$
29.613	29.496	29.461	29.460	29.456	29.456
20.094	20.048	20.039	20.030	20.028	20.028
0.960	1.091	1.168	1.2790	1.264	1.257
0.706	0.760	0.788	0.8610	0.851	0.845
0.234	0.175	0.052	0.0085	0.0154	0.026
0.209	0.160	0.046	0.0074	0.0125	0.022
0.106	0.078	0.024	0.0045	0.0031	$10^{-12}$
0.075	0.058	0.021	0.0031	0.0025	$10^{-12}$
0.073	0.057	0.021	0.0023	0.0020	$10^{-13}$
0.072	0.056	0.020	0.0014	0.0014	$10^{-13}$
0.069	0.055	0.020	0.0013	0.0013	$10^{-13}$
0.066	0.050	0.017	0.0012	0.0012	$10^{-13}$

The results presented in Tables (5) and (6) indicate that the combined algorithm is capable of identifying modes with amplitudes as low as 1% of the noise. In each case, we have assumed the minimum model identified by the first pass of the ERA. Thus, for example, at  $\sigma = 0.1$ , which is twice the amplitude of mode 2 and 100 times the amplitude of mode 3, the ERA algorithm identifies a single mode. Using only this one-mode model as input to the MME, the combined algorithm is still able to determine that the true model order is three, and give good accuracy in the parameter estimates.

Table 6. Parameter identification from the ERA/MME algorithm.

Noise	Mode 1		Mode 2		Mode 3	
	Frequency	Damping	Frequency	Damping	Frequency	Damping
$\sigma = 0.1$	0.996	$1.44 \times 10^{-3}$	2.910	$-4.09 \times 10^{-2}$	5.408	-0.408
$\sigma = 0.05$	0.998	$4.14 \times 10^{-4}$	2.827	$-7.97 \times 10^{-3}$	5.517	-0.554
$\sigma = 0.01$	0.999	$-7.18 \times 10^{-5}$	2.768	$2.22 \times 10^{-3}$	5.678	-0.766
$\sigma = 0.003$	1.000	$-4.30 \times 10^{-5}$	2.766	$-1.62 \times 10^{-3}$	5.589	-0.142
$\sigma = 0.001$	1.000	$-4.61 \times 10^{-5}$	2.763	$2.00 \times 10^{-4}$	5.397	0.044
True	1.000	0	2.760	0	5.400	0

#### 5.4 Sample Comparison With Extended Kalman Filter-Smoother

To illustrate the potential advantages of the model error terms in the MME compared with process noise in filters, consider the following nonlinear problem. The truth is given by the equation

$$\dot{x} = -\frac{x + t^2}{2x + t} \quad (22)$$

For illustration, the assumed model for the estimation algorithms is

$$\dot{x} = 0 \quad (23)$$

The measurements are perfect measurements of  $x$ . The MME is applied to this problem, and, for comparison, an extended Kalman filter-smoother is also used. The EKFS is modeled after the well-known Rauch-Tung-Streibell<sup>21</sup> filter-smoother, extended for the nonlinear problem. Since the assumed model is zero, the EKFS estimate must be constant between the measurements. The results of the two estimation approaches are shown in Figure (17). The model correction capability of the MME enables it to produce state estimates using a corrected version of the original model, so that the MME is not constant between measurements. The advantage of this approach is clear in Figure (17). Even though the measurements are perfect, the EKFS estimates between the measurements are poor.

### Summary and Conclusions

In this paper, a new method for optimal post-experiment estimation has been described and its application demonstrated by numerous examples. The method is formulated to account for model error in a much more general and rigorous fashion than the process noise assumptions of typical filter algorithms. The state estimates are continuous and based on global measurement fits, compared with filter estimates which are discrete and based on local measurement fits. The MME method may give vastly improved state estimates when compared with filters for dynamic problems with significant model error, especially if the measurements are sparse and/or noisy.

In the MME, model error is treated as an unknown and estimated along with the states. The estimated model error is automatically corrected in the original model in order to obtain the state estimates. For poorly modeled systems, this produces two significant benefits. First, the state

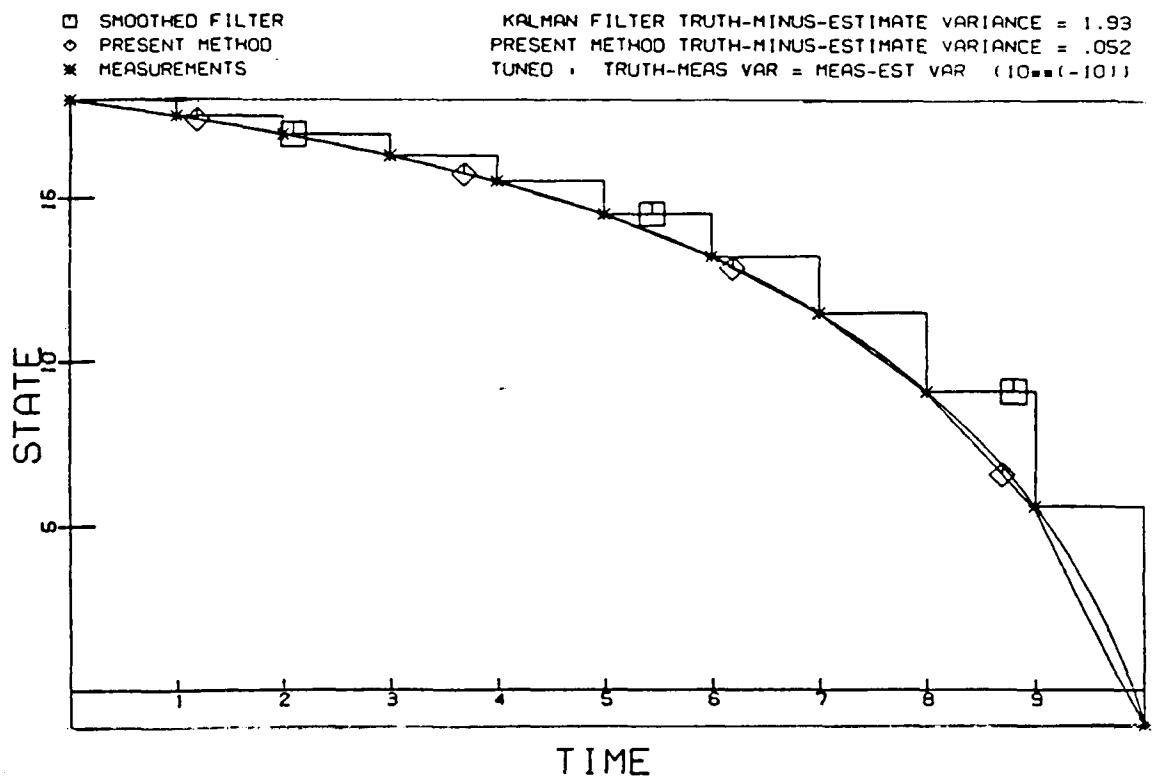


Figure 17. Comparison of the MME with an extended Kalman filter-smoother in the absence of a model. The EKFS estimate must be constant between measurements, but the model correction in the MME shows clear advantages.

estimates are based on a corrected model (unlike filters), and second, the model error estimates are available to aid in identification of an accurate model for subsequent use.

Examples are given which demonstrate state estimation and exploitation of the model error estimates for both system identification and external force identification. The MME method shows considerable promise for use in numerous post-experiment estimation and identification problems, and should be considered for any application in which significant model error is suspected.

## REFERENCES

1. Gelb, A., editor, Applied Optimal Estimation, MIT Press, Cambridge, Massachusetts, 1984.
2. Fitzgerald, R. J., "Divergence of the Kalman Filter," IEEE Transactions on Automatic Control, Vol. AC-16, p. 736, 1971.
3. Huber, P. J., "The 1972 Wald Lecture: Robust Statistics: A Review," Annals of Mathematical Statistics, Vol. 43, p. 1041, 1972.
4. Breza, M. J., and Bryson, A. E., "Minimum-Variance Steady-State Filters With Eigenvalue Constraints", 5th Symposium on Nonlinear Estimation Theory and its Applications, San Diego, 1974.
5. Mook, D.J., and Junkins, J.L., "Minimum Model Error Estimation for Poorly Modeled Dynamic Systems", AIAA Journal of Guidance, Control, and Dynamics, to appear.
6. Geering, H.P., "Continuous-Time Optimal Control Theory for Cost Functionals Including Discrete State Penalty Terms", IEEE Transactions on Automatic Control, Volume AC-21, pp. 866-869, 1976.
7. Rozonoer, L.I., "L.S. Pontryagin Maximum Principle in Optimal System Theory", Avtomat. I. Telemekh, Vol. 20, 1959. Also in Optimal and Self-Optimizing Control, R. Oldenburger, editor, MIT Press, 1966.
8. Lew, J.S., and Mook, D.J., "Two-Point Boundary Problems Containing Jump Discontinuities", in review.
9. Mook, D.J., and Lin, J.-C., "Minimum Model Error Estimation of Modal Truncation Errors", Proceedings of the 1987 Spring Meeting of the Society for Experimental Mechanics, Houston, TX, June 1987.
10. Lin, J. C., "Minimum Model Error Estimation of Modal Truncation Errors", M.S. Thesis, State University of New York at Buffalo, 1988.
11. Mook, D.J., "Estimation and Identification of Nonlinear Dynamic Systems", Proceedings of the 29<sup>th</sup> Structures, Structural Dynamics, and Materials Conference, Williamsburg, Virginia, April 1988. Also, to appear, AIAA Journal.
12. Thompson, J. M. T., and Stewart, Nonlinear Dynamics and Chaos, John Wiley and Sons, 1986.
13. Mook, D. J., Liu, S.-A., and Ho, F.-S., "Linear Model Parameter Identification From State Measurements", Proceedings of the 18<sup>th</sup> Annual Pittsburgh Conference on Modeling and Simulation, Pittsburgh, April 1987.
14. Ibrahim, S.R., and Mikulcik, E.C., "A Method for the Direct Identification of Vibration Parameters from the Free Response," Shock and Vibration Bulletin, No. 47, Pt. 4, pp. 183-198, Sept. 1977.
15. Rajaram, S., and Junkins, J.L., "Identification of Vibrating Flexible Structures", AIAA Journal of Guidance, Control, and Dynamics, Vol. 8, No. 4, pp. 463-470, July-Aug. 1985.

16. Hendricks, S.L., et. al., "Identification of Mass, Damping, and Stiffness Matrices for Large Linear Vibratory Systems", *AIAA Journal of Guidance, Control, and Dynamics*, Vol. 7, No. 2, pp. 244-245, March-April 1984.
17. Chen, J.C., et.al., "Direct Structural Parameter Identification by Modal Test Results", 24th Structures, Structural Dynamics, and Materials Conference, Pt. 2, 1983.
18. Juang, J.-N., and Pappa, R.S., "An Eigensystem Realization Algorithm (ERA) for Modal Parameter Identification and Model Reduction", *AIAA Journal of Guidance, Control, and Dynamics*, Vol. 8, No. 5, pp. 620-627, Sept.-Oct. 1985.
19. Juang, J.N., and Pappa, R.S., "Effects of Noise on Modal Parameters Identified by the Eigensystem Realization Algorithm", *AIAA Journal of Guidance, Control, and Dynamics*, Vol. 9, No. 3, pp. 294-303, May-June 1986.
20. Mook, D. J., and Lew, J., "A Combined ERA/MME Algorithm For Robust System Realization/Identification", *AIAA/ASME/ASCE/AHS 29<sup>th</sup> Structures, Structural Dynamics, and Materials Conference*, Williamsburg, Virginia, April 1988.
21. Rauch, H. E., Tung, F., and Streibel, C. T., "Maximum Likelihood Estimates of Linear Dynamic Systems", *AIAA Journal*, Vol. 3, No. 8, pp. 1445-1450, 1965.